Electronic Supplementary Material (ESM)

Supplementary Methods

Radiocarbon dating

Cores, representing either disturbed (single core: Disturbed 1 – D1) or undisturbed (two cores: Undisturbed 1 and 2 – U1 and U2) conditions, were dated (Table 1). Shell samples were selected from the cores for dating. For the undisturbed core, both a shell and a charcoal fragment were extracted from 100 cm depth for dating. The surface of the shell samples were cleaned using either a dremel drill for large shells, or etched in dilute HCl (0.5 M), and the shells washed in deionized water, and dried at 60°C overnight. The shells (between 12.24 mg – 20.24 mg) were placed in sealed, evacuated vials and reacted with excess phosphoric acid at 60°C overnight. The charcoal was pretreated using HCl (2M), NaOH (2%, 4 times) and HCl (2M) to remove humic and fulvic acid contaminants. The charcoal was washed thoroughly with Milli-Q water and dried at 60°C overnight. An aliquot (3.46 mg) of the charcoal was oxidised in an evacuated, sealed silica tube using copper oxide with silver and copper wire and heated to 900°C. The resulting CO_2 was purified cryogenically and the carbon yield determined manometrically (yields between 0.20 mg C - 0.41 mg C) and graphitized via reduction with H_2 over an Fe catalyst at 600°C (Hua et al. 2001) to form a graphite target for AMS measurement. The graphite target was measured on the STAR accelerator (HVE 2MV Tandetron), with all measurements normalized against the oxalic acid (HOXI) international standard. For each sample ^{14}C concentration and/or radiocarbon age was determined after corrections for AMS machine background, procedural blank and isotopic fractionation using the $\delta^{13}C$ of the graphite which was obtained by analysis using an elemental analyser isotope ratio mass spectrometer (EA-IRMS, vario Micro cube EA, Elementar Germany and IsoPrime IRMS, GV Instruments, UK) (Fink et al. 2004). ^{14}C concentration is reported as percent modern carbon (pMC) and ages as conventional radiocarbon age (yrs BP). The calendar ages were obtained by calibrating the radiocarbon ages using the OxCal v4.2 programme (Ramsey 2009). Shell samples were calibrated against the Marine13 dataset (Reimer et al. 2013) using a regional ΔR determined from a charcoal/shell pair collected from the same depth. The charcoal sample was calibrated against the SHCal13 dataset (Hogg et al. 2013).

16S rRNA sequencing and bioinformatics for determining bacterial community composition

DNA was extracted from 1 g of sediment PowerSoil DNA Isolation Kit (MO BIO Laboratories). The 16S rRNA gene V1-V3 variable regions were amplified using the 16S rRNA Eubacterial primers 27F (5'-AGAGTTTGATCCTGGCTCAG-3') and 519R (5′GTATTACCGCGGCKGCTG-3′) and a 30 cycle PCR using the HotStarTaq Plus Master Mix Kit (Qiagen, USA) under the following conditions: 94°C for 3 minutes, followed by 28 cycles of 94°C for 30 seconds, 53°C for 40 seconds and 72°C for 1 minute, after which a final elongation step at 72°C for 5 minutes was performed. PCR products were purified using Agencourt Ampure XP beads (Agencourt Bioscience Corporation, USA) and used to prepare a DNA library by following Illumina TruSeq DNA library preparation protocol. Sequencing was performed on the Illumina MiSeq platform (www.mrdnalab.com, Shallowater, TX, USA) following the manufacturer's guidelines. Only a subset of replicates were able to be successfully sequenced for further bacterial taxonomic analysis (disturbed n=5, recovered n=3, undisturbed n=3).

Bacterial samples were processed using the QIIME package (Caporaso et al. 2010). Following sequencing, barcodes were removed from the sequences, sequences shorter than 150bp were removed and sequences with ambiguous base calls were removed. Paired ends were joined and chimeras removed using USEARCH. Operational taxonomic units (OTUs) were defined as sequences sharing 97% similarity using UCLUST. Samples were rarefied to 9153 sequences to ensure even sampling depth. Representative sequences of each OTU were compared against the Greengenes database (http://greengenes.lbl.gov/cgi-bin/nph-index.cgi) (DeSantis et al. 2006) using BLAST ($E<10^{-5}$) (Altschul et al. 1997) to assign taxonomy. Metagenomes were also predicted for the bacterial samples using the PICRUSt package (Langille et al. 2013). The QIIME package was used to pick closed-referenced OTUs against the Greengenes database at 97% similarity. OTUs were normalized by copy number and rarefied at 3401 sequences before metagenomes were predicted for levels 2 and 3 of KEGG pathways.

Supplementary Results

Carbon ages

The radiocarbon ages for the sediment samples are reported in Supplementary Table 1. A regional marine reservoir correction, ΔR, was determined from the charcoal/shell pair from 100 cm depth from core U1 (samples OZ R657 and OZR653), following the method described in Weisler et al. (2009) and Russell et al. (2011). The charcoal provided the terrestrial/atmospheric radiocarbon age for the core at 100 cm depth, the corresponding marine age of this charcoal was determined by interpolating between the SHCal13 curve and the Marine13 curve to give a modelled marine age. ΔR is then calculated as the difference between the measured marine age (of the shell) and the modelled marine age (for the charcoal). The associated 1σ error for ΔR was calculated as per Weisler et al. (2009), $(\sigma_{\text{measured age}}^2 + \sigma_{\text{modelled age}}^2)^{1/2}$. For each core, there is a sequential progression in age down the core. Core U1 (undisturbed) was the deepest core, and gave the oldest mean calibrated age of 6,476 ± 164 yrs cal BP at 100 cm depth. The top of this core was Modern (younger than 1955) at 7 cm, as indicated by the radiocarbon content of 106.83 ± 0.24 pMC which shows the influence of radiocarbon resulting from above ground nuclear testing which occurred during the late 1950s and early 1960s (Nydal 1968; Hua et al. 2013). As this is a marine sample affected by this 'bomb carbon' this measurement could not be calibrated to a calendar age. Assuming a constant rate of deposition over time, the sedimentation rate for this core is 0.015 cm yr^{-1}. Core U2 is shorter, with a basal mean calibrated age of 2,115 ± 188 yrs cal BP, and shows a faster sedimentation rate of 0.028 cm yr^{-1}. Core D1 represents the disturbed areas. With a basal mean calibrated age of 5,232 ± 224 cal yrs BP at 68 cm depth, this core has a sedimentation rate of 0.017 cm yr^{-1}, similar to that of core U1. Interestingly, the top of D1 gave an age of 288 ± 174 cal yrs BP at 5 cm depth, markedly different to that of U1, which had a Modern age at 7 cm depth. It is possible that the seismic disturbance had removed the surface of this area.

Bacterial responses

ANOSIM analysis and MDS plot for PICRUSt showed similar trends as the community data, except for an outlier in which one disturbed replicate clustered more closely with the undisturbed samples (Supplementary Fig. S3). Removal of this data point did not alter the SIMPER trends but ANOSIM analysis between disturbed and undisturbed changed from marginally significant ($R = 0.549$, $P = 0.055$) to significant ($R = 1$, $P = 0.029$).

Supplementary References

Altschul SF, Madden TL, Schaffer AA, Zhang JH, Zhang Z, Miller W, Lipman DJ (1997) Gapped BLAST and PSI-BLAST: a new generation of protein database search programs. Nucleic Acids Res 25: 3389-3402 doi 10.1093/nar/25.17.3389

Caporaso JG, Kuczynski J, Stombaugh J, Bittinger K, Bushman FD, Costello EK, Fierer N, Pena AG, Goodrich JK, Gordon JI, Huttley GA, Kelley ST, Knights D, Koenig JE, Ley RE, Lozupone CA, McDonald D, Muegge BD, Pirrung M, Reeder J, Sevinsky JR, Tumbaugh PJ, Walters WA, Widmann J, Yatsunenko T, Zaneveld J, Knight R (2010) QIIME allows analysis of high-throughput community sequencing data. Nat Meth 7: 335-336 doi 10.1038/nmeth.f.303

DeSantis TZ, Hugenholtz P, Larsen N, Rojas M, Brodie EL, Keller K, Huber T, Dalevi D, Hu P, Andersen GL (2006) Greengenes, a chimera-checked 16S rRNA gene database and workbench compatible with ARB. Appl Environ Microbiol 72: 5069-5072 doi 10.1128/aem.03006-05

Fink D, Hotchkis M, Hua Q, Jacobsen G, Smith AM, Zoppi U, Child D, Mifsud C, van der Gaast H, Williams A, Williams M (2004) The ANTARES AMS facility at ANSTO. Nuclear Instruments & Methods in Physics Research Section B-Beam Interactions with Materials and Atoms 223: 109-115 doi 10.1016/j.nimb.2004.04.025

Hogg AG, Hua Q, Blackwell PG, Niu M, Buck CE, Guilderson TP, Heaton TJ, Palmer JG, Reimer PJ, Reimer RW, Turney CSM, Zimmerman SRH (2013) SHCAL13 Southern hemisphere calibration, 0-50,000 years cal BP. Radiocarbon 55: 1889-1903

Hua Q, Barbetti M, Rakowski AZ (2013) Atmospheric radiocarbon for the period 1950-2010. Radiocarbon 55: 2059-2072

Hua Q, Jacobsen GE, Zoppi U, Lawson EM, Williams AA, Smith AM, McGann MJ (2001) Progress in radiocarbon target preparation at the ANTARES AMS Centre. Radiocarbon 43: 275-282

Langille MGI, Zaneveld J, Caporaso JG, McDonald D, Knights D, Reyes JA, Clemente JC, Burkepile DE, Thurber RLV, Knight R, Beiko RG, Huttenhower C (2013) Predictive functional profiling of microbial communities using 16S rRNA marker gene sequences. Nat Biotechnol 31: 814-+ doi 10.1038/nbt.2676

Lebaron P, Servais P, Agogue H, Courties C, Joux F (2001) Does the high nucleic acid content of individual bacterial cells allow us to discriminate between active cells and inactive cells in aquatic systems? Appl Environ Microbiol 67: 1775-1782 doi 10.1128/aem.67.4.1775-1782.2001

Macreadie PI, Allen K, Kelaher BP, Ralph PJ, Skilbeck CG (2012) Paleoreconstruction of estuarine sediments reveal human-induced weakening of coastal carbon sinks. Global Change Biology 18: 891-901 doi 10.1111/j.1365-2486.2011.02582.x

Marie D, Partensky F, Jacquet S, Vaulot D (1997) Enumeration and cell cycle analysis of natural populations of marine picoplankton by flow cytometry using the nucleic acid stain SYBR Green I. Applied and Environmental Microbiology 63: 186-193

Nydal R (1968) Further investigation on the transfer of radiocarbon in nature. J Geophys Res 73: 3617-3635

Ramsey CB (2009) Bayesian analysis of radiocarbon dates. Radiocarbon 51: 337-360

Reimer PJ, Bard E, Bayliss A, Beck JW, Blackwell PG, Ramsey CB, Buck CE, Cheng H, Edwards RL, Friedrich M, Grootes PM, Guilderson TP, Haflidason H, Hajdas I, Hatte C, Heaton TJ, Hoffmann DL, Hogg AG, Hughen KA, Kaiser KF, Kromer B, Manning SW, Niu M, Reimer RW, Richards DA, Scott EM, Southon JR, Staff RA, Turney CSM, van der Plicht J (2013) INTCAL13 and MARINE13 radiocarbon age calibration curves 0-50,000 years cal BP. Radiocarbon 55: 1869-1887

Russell N, Cook GT, Ascough PL, Scott EM, Dugmore AJ (2011) Examining the inherent variabilty in Delta R: New methods of presenting Delta R values and implications for MRE studies. Radiocarbon 53: 277-288

Seymour JR, Seuront L, Mitchell JG (2007) Microscale gradients of planktonic microbial communities above the sediment surface in a mangrove estuary. Estuar Coast Shelf Sci 73: 651-666 doi 10.1016/j.ecss.2007.03.004

Trevathan-Tackett S, Macreadie P, Ralph P, Seymour J (2014) Detachment and flow cytometric quantification of seagrass-associated bacteria. Journal of Microbial Methods 102: 23-25

Weisler MI, Hua Q, Zhao J-x (2009) Late Holocene 14C marine reservoir corrections for Hawai'i derived from U-series archaelogical coral. Radiocarbon 51: 955-968

Supplementary Figures

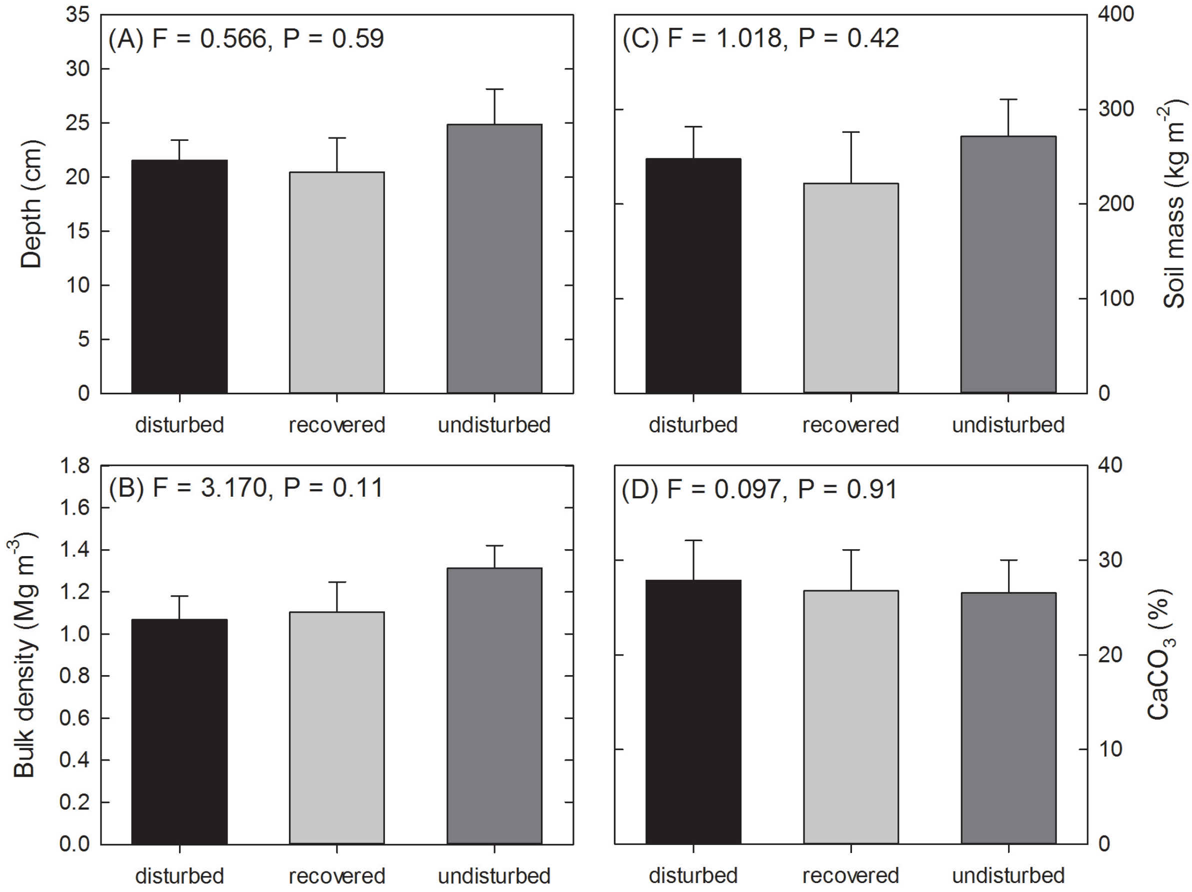

Supplementary Figure S1: Differences in mean core depth, dry bulk density, soil mass or carbonate content among the disturbed, recovered and undisturbed habitats.

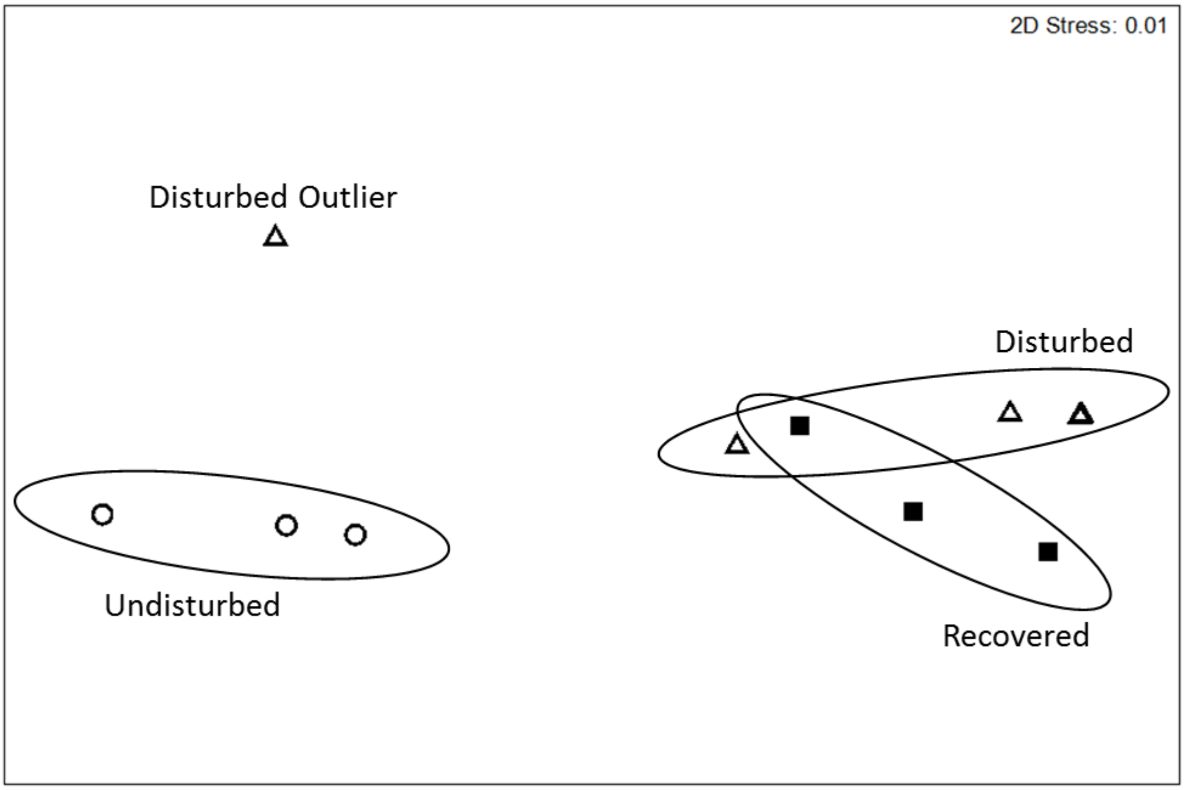

Supplementary Figure S3. MDS plot showing clustering of predicted metagenomes using PICRUSt analysis across disturbed, recovered, and undisturbed sediments.

Supplementary Tables

Supplementary Table S1. Soil ages. Radiocarbon ages (^{14}C dates) derived from sediments taken from two habitat types: Disturbed (D) or Undisturbed (U) seagrass.

ANSTO code	Sample Type	Habitat and core number (Depth)	percent Modern Carbon pMC±1σ error	Conventional Radiocarbon Age yrs BP±1σ error	Calibrated Age Range Cal BP (95.4% probability)	Mean Calibrated Age Cal BP±2σ error
OZR647	shell	D2 (5 cm)	93.61± 0.25	530±25	452-118	288±174
OZR648	shell	D2 (37 cm)	69.48± 0.23	2925±30	2990-2692	2826±154
OZR649	shell	D2 (72 cm)	56.74± 0.22	4550±35	5172-4702	4914±200
OZR650	shell	D2 (89 cm)	54.98± 0.21	4805±35	5444-5023	5232±224
OZR651	shell	U1 (7 cm)	106.83±0.24	NA	NA	NA
OZR652	shell	U1 (80 cm)	49.04±0.19	5725±35	6418-6090	6255±158
OZR653	shell	U1 (100 cm)	47.77±0.18	5935±35	6638-6303	6476±164
OZR654	shell	U2 (20 cm)	94.75±0.25	435±25	293-0	168±164
OZR655	shell	U2 (38 cm)	84.98±0.25	1310±25	1147-815	978±158
OZR656	shell	U2 (60 cm)	74.68±0.19	2345±25	2295-1942	2115±188
OZR657	Charcoal	U1 (100 cm)	49.00±0.22	5730±40	6631-6353	6476±116

Supplementary Table S2. Top contributing genes and abundances between undistrubed and disturbed sites from SIMPER analysis for Level 2 and 3 Kegg Pathways. Outlier not included (see text).

KEGG: Level 2	Average Abundance		Mean	%
Pathway	Undisturbed	Disturbed	Dissimilarity	Contribution
Cell Motility	0.17	0.15	0.22	13.74
Energy Metabolism	0.28	0.3	0.19	12.09
Lipid Metabolism	0.19	0.18	0.1	6.2
Metabolism of Cofactors and Vitamins	0.22	0.23	0.09	5.65
Enzyme Families	0.15	0.16	0.07	4.75
Amino Acid Metabolism	0.31	0.3	0.07	4.43

KEGG: Level 3	Average Abundance		Mean	%
Pathway	Undisturbed	Disturbed	Dissimilarity	Contribution
Photosynthesis proteins[1]	0.12	0.14	0.08	3.22
Photosynthesis[1]	0.11	0.13	0.07	2.74
Flagellar assembly[2]	0.07	0.05	0.06	2.55
Bacterial chemotaxis[2]	0.07	0.05	0.06	2.39
Bacterial motility proteins[2]	0.13	0.12	0.05	1.9
Photosynthesis - antenna proteins[1]	0.05	0.06	0.04	1.72

[1]Energy Metabolism
[2]Cell Motility